

# Stratification observed by the in situ plasma density measurements from the Swarm satellites

Xiuying Wang<sup>1</sup>, Wanli Cheng<sup>2</sup>, Zihan Zhou<sup>1</sup>, Dehe Yang<sup>1</sup>, Jing Cui<sup>1</sup>, Feng Guo<sup>1</sup>

1) Institute of Crustal Dynamics, China Earthquake Administration, Beijing, China

2) Xinyang Station, Henan Earthquake Administration, Henan, China

Corresponding author: Xiuying Wang (652383915@qq.com)

Key Points:

- First application of in situ plasma densities for the direct analysis of the stratification in F2 layer.
- Refined features of exact location and continuous morphology for the stratification phenomenon.
- A new discovery of stratification covering all longitudes in southern mid-latitudes.

Abstract: Stratification phenomenon is investigated using the simultaneous in situ plasma density measurements obtained by the Swarm satellites orbiting at different altitudes above F2 peak. For the first time, the continuous distribution morphology and the exact locations are obtained for the nighttime stratification, which show that the stratification events are centered at the EIA (equatorial ionization anomaly) trough and extend towards the two EIA crests with the most significant part being located at the EIA trough. Another new discovery is the stratification in southern mid-latitudes; stratification events in this region are located on a local plasma peak sandwiched by two lower density strips covering all the longitudes. The formation mechanism of the stratification for the two latitudinal regions is discussed, but the stratification mechanism in southern mid-latitudes remains an unsolved problem.

Key words: stratification, ionospheric F2 layer, in situ plasma density, Swarm satellites, southern mid-latitudes stratification, stratification morphology

## 1. Introduction

Stratification is a kind of phenomenon appearing in the ionospheric F2 layer at low-latitudes near geomagnetic equator, where additional layer is shown above the F2 layer peak due to the combined effect of the upward  $E \times B$  drift at the geomagnetic equator and the meridional neutral wind (Balan et al., 1997, 1998; Jenkins et al, 1997). This additional layer was called G layer and renamed to F3 layer by Balan et al. (1997) due to its same chemistry as the F region.

Since stratification was first reported in the mid-20th century (Sen, 1949; Skinner et al., 1954), many studies have been conducted to study the formation mechanism, diurnal, seasonal and solar activity dependence of this phenomenon using different measurements, such as ground-based ionospheric sounding ionograms (Balan et al., 1997; Batista et al., 2002; Jenkins et al., 1997; Zhao et al., 2011a), ground-based TEC (Thampi et al., 2005), satellite-based ionospheric sounding ionograms (Depuev and Pulinets, 2001; Karpachev et al., 2013; Lockwood and Nelms, 1964), satellite-based radio occultation (RO) observations (Zhao et al., 2011b), satellite-based in situ measurements (Wang et al., 2019). All these studies have shown that stratification above F2 peak is a regular rather than an anomalous phenomenon appearing both during the day and at night and is limited in a narrow zone near the geomagnetic equator regions, and the occurrence of this stratification phenomenon depends on season, solar activity and geomagnetic activity (Balan et al.,

1 2008; Batista et al., 2002; Jenkins et al., 1997; Zhao et al., 2011a).

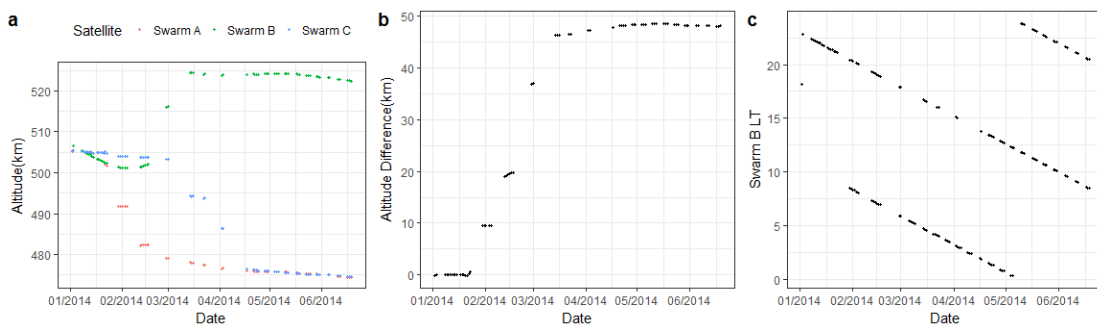
2 The features and formation mechanism of the ionospheric F2 layer stratification have been  
3 extensively investigated for several decades, but unsolved problems, such as the exact locations and  
4 distribution morphology that are useful to understand this phenomenon, still exist due to the  
5 scattered and limited spatial coverage of the observations used in previous studies. So far, most of  
6 these studies are based on ground-based or satellite-based ionograms. For the former, stratification  
7 can only be observed during the period when the peak density of the stratification layer exceeds that  
8 of the F2 layer; and for the latter, only during the period when the peak density of the stratification  
9 layer is lower than the F2 peak. Continuous global distribution of the stratification cannot be  
10 obtained from these scattered observations though local season and solar activity dependence  
11 features can be obtained from these long-term observations. Moreover, there are contradictory  
12 results in these studies. Whereas, simultaneous satellite-based in situ observations at different  
13 altitudes above the F2 layer peak can provide spatial coverage of more extensive region, which can  
14 incorporate all local time and longitudes. And the most important is that the morphology of the  
15 stratification along the latitudinal direction can be obtained using the continuous measurements.

16 In this paper, for the first time, the in situ plasma measurements from the Swarm satellites are  
17 used to study the precise locations, distribution and morphology of the stratification phenomenon.  
18 Nighttime stratification on the southern mid-latitudes is found, which is never mentioned in previous  
19 studies. Our results can provide new perspective for the stratification phenomenon, which is helpful  
20 to the insight of the ionospheric F2 layer.

## 21 2. Data and method

22 Swarm, launched on 22 November 2013 by the European Space Agency (ESA), is a constellation  
23 mission comprising three identical satellites (A, B & C). The three satellites are placed in two  
24 different polar orbits, two flying side by side (A & C) at an altitude of about 460km with longitudinal  
25 separation of about 1.4°, and a third (B) at an altitude of about 510km (Knudsen et al, 2017).  
26 Consistent in situ plasma densities are measured by the Langmuir probes (LP) onboard the three  
27 Swarm satellites with a time resolution of 2Hz (Lomidze et al, 2018).

28 The three satellites began to separate in altitudes from the end of January 2014 and the separation  
29 operations were completed in April 2014, as shown in Fig. 1. During and immediately after the  
30 separation operations, the three satellites orbit at similar local time and similar locations in different  
31 altitudes above the F2 peak region, which provides a good opportunity to check and understand the  
32 distribution and morphology of the F2 layer stratification phenomenon using simultaneous in situ  
33 measurements obtained on a global scale.

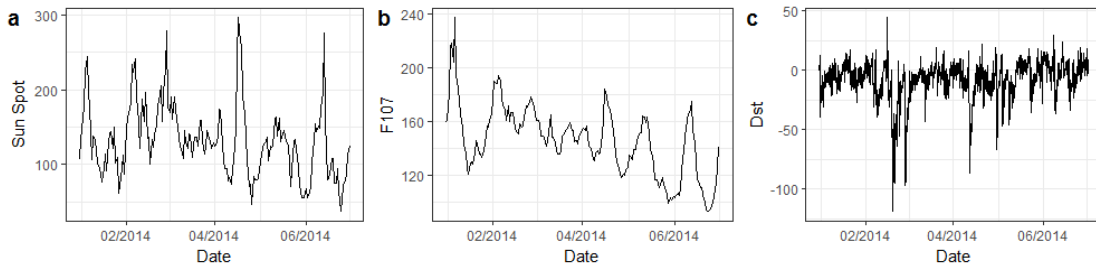


34  
35 Fig. 1 Variations of orbiting parameters with time

1 ((a) Variations of orbiting altitude of the three satellites with time; (b) Variations of altitude difference between  
 2 Swarm B and A with time; (c) Variations of Swarm B LT with time. The orbiting altitude, altitude difference, and  
 3 Swarm B LT in (a), (b), and (c) indicate the daily average values near the geographical Equator.)

4 Separation of the three satellites follow different schemes as shown in Fig. 1(a). To simplify the  
 5 calculation, we use only the measurements from Swarm A and B as the two satellites are closer to  
 6 each other, and they have more co-located orbit tracks after altitude separation. Therefore, co-  
 7 located in situ plasma density measurements from Swarm A and B are selected using the criteria  
 8 defined below to conduct this study.

9 We also give the solar and geomagnetic activity indices during the select period, as shown in  
 10 Fig.2. According to Fig.2(a) and (b), the solar activity during the selected period is medium. Since  
 11 there are few geomagnetic events as shown in Fig.2(c), we won't distinguish the data into disturbed  
 12 and undisturbed cases here. Therefore, all the selected co-located orbit pairs are used in this study.



13  
 14 Fig. 2 Variations of solar and geomagnetic indices with time

15 ((a) Variations of Sun spot index with time; (b) Variation of F10.7 index with time; and (c) Variation of Dst index  
 16 with time.)

17 To detect stratification events, measurements of the co-located orbit pairs from the two satellites  
 18 are compared directly. Spatial and temporal criteria to search co-located orbit tracks are defined as:  
 19 (1) longitude difference between two orbit tracks near the equator region is within  $5^\circ$ , which can  
 20 keep true for nearly all the mid-latitudes as the orbit tracks of the Swarm satellites are almost parallel  
 21 to longitude for mid- and low-latitudes. This  $5^\circ$  spatial difference in longitude direction is  
 22 reasonable because of the little and negligible variation of the ionosphere in a small spatial scale.  
 23 According to Shim et al. (2008), the longitudinal correlation can vary from  $23^\circ$  at mid-latitudes  
 24 and  $15^\circ$  at low-latitudes during the day to  $11^\circ$  at mid-latitudes and  $10^\circ$  at low latitudes during the  
 25 night; and (2) time difference of measurements at similar latitude between two orbits is less than 30  
 26 min as appearance of stratification is normally much longer than this criterion (Balan et al., 1997);  
 27 moreover, variations of electron densities within 30 minutes can be neglected comparing to the  
 28 diurnal variation under geomagnetic quiet conditions.

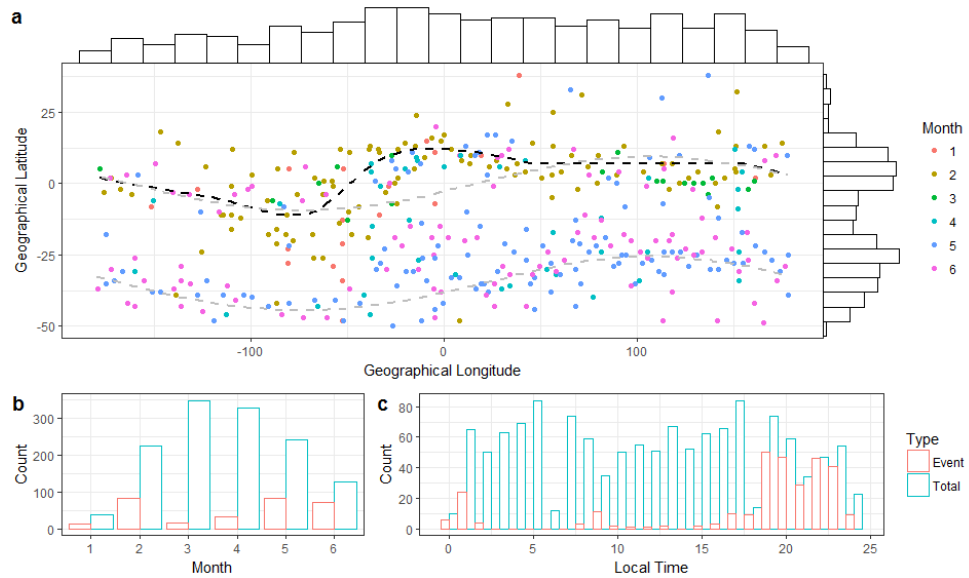
29 A search of the dataset from Swarm A and B using the criteria, 1313 matched orbit pairs are found  
 30 from January to June 2014. Here, matched orbits indicate ascending (from south to north) or  
 31 descending (from north to south) half orbit tracks as a satellite passes the same location twice a day,  
 32 corresponding to daytime and nighttime respectively, as shown in Fig.1(c), which gives the local  
 33 time (LT) of Swarm B for both ascending and descending orbit during the selected data period.

34 Using these co-located orbit pairs, stratification events are identified by the following process. (1)  
 35 In situ plasma density measurements along the orbit tracks are down-sampled by averaging the data  
 36 over  $1^\circ$  latitude range; (2) The down-sampled data at same latitude from the two satellites are  
 37 compared, then data points, where average plasma density from Swarm B is greater than that from  
 38 Swarm A, are picked out; (3) Stratification events are identified only when at least 5 continual data

1 difference (Swarm B minus Swarm A) points are positive, which means a continual latitude of at  
 2 least  $5^\circ$ . Adoption of continual  $5^\circ$  at latitudinal direction is because the auto-detecting process may  
 3 make wrong decisions if less data points are considered due to the small data fluctuations of the  
 4 observations. Some very small stratification may be discarded in this way, but it won't affect the  
 5 final results. After all the stratification events are determined, the morphology along the latitude,  
 6 the location, and the global distribution of the stratification events are then studied based on the  
 7 detected events.

8 **3. Results**

9 The global distribution of the detected stratification events from all the co-located orbit pairs from  
 10 January to June 2014 is given in Fig. 3, also given in this figure is the variations of the occurrence  
 11 number with local time and month. As more than one event may be detected from one orbit track,  
 12 Fig. 3(a) plots all the detected stratification events, but only one event is counted per orbit track in  
 13 Fig.3(b) and (c) when comparing the statistical results. The location of each stratification event is  
 14 identified as the place where maximum data difference is located, and the color of each point  
 15 represents occurrence month of that event.



16  
 17 **Fig. 3** Distribution of detected stratification events and variations of occurrence number with local time and month  
 18 (In (a), each point represents a stratification event, and the location of each point indicates the position of the maximum data difference  
 19 of that detected event. Color of each points indicates the occurrence month of the stratification event. Grey dash line indicates the  
 20 geomagnetic equator and  $35^\circ$  S geomagnetic latitude under dipole coordinates, and black dash line indicates dip equator. In (b) and (c),  
 21 'Event' indicates detected stratification events, 'Total' indicates total co-located orbit number.)As shown in Fig. 3(c), most of  
 22 the detected stratification events are mainly concentrated during 18:00 to 01:00 LT, with 18:00 to  
 23 23:00 LT being the most clustered period. In contrast, daytime stratification events are fewer, which  
 24 is quite different from those studies that stratifications are concentrated from morning to noon period  
 25 (Balan et al., 1998; Batista et al., 2002; Rama Rao et al., 2005). As to the seasonal variations in  
 26 Fig.3(b), the most frequent occurrence of the stratification is in January, February, May and June  
 27 when comparing to the total number of co-located orbit pairs. The lower event number in January  
 28 is because the altitudes separation began at the end of this month, its occurrence rate (detected events  
 29 divide by total) is comparable to that in February, May, and June. As to the very small event number

1 in March and April, it is necessary to point out that the local time of the two satellites coincides to  
2 dawn and dusk during these two months, as shown in Fig.1(c), which may be the reason why  
3 detected events are fewer during this period. Fewer stratification events during March and April is  
4 consistent with the fewer events during the day, which we will discuss in Section 4.

5 It can be seen clearly from Fig.3(a) that stratification events are concentrated on two geomagnetic  
6 latitudes, one is the geomagnetic equator region, where most previous studies are concentrated on;  
7 and the other is the mid-latitude region on the Southern Hemisphere, where the distribution of the  
8 stratification events also show the feature of being parallel to the geomagnetic equator. It should be  
9 noted here that the geomagnetic equator and latitude shown by grey dash line in Fig.3(a) are from  
10 dipole coordinates, and dip equator shown by black dash line is also given as a comparison.  
11 Geomagnetic control of the stratification events in southern mid-latitudes is obviously shown  
12 according to its distribution feature. In Fig.3(a), stratification events near the geomagnetic equator  
13 can occur in each month from January to June, whereas stratification on the southern mid-latitudes  
14 only occur in May and June, just the local winter.

15 As to the longitudinal distribution, stratification events can cover all longitudes, generally  
16 showing a slightly denser distribution in the eastern hemisphere than in the western hemisphere,  
17 which may be related to the limited statistical data. The all longitude coverage feature is consistent  
18 with the results from Zhao et al. (2011b). A longitudinal peak is shown between longitude (-50,0)  
19 in Fig.3(a), though it is not very obvious. This longitude peak coincides with the region where the  
20 dip equator, the black dash line in Fig.3(a), transits from the south to the north of geographical  
21 equator. This region is also the place where the ground-based sounding observations are used by  
22 many previous studies (Balan et al., 1998; Batista, 2001; Jenkins et al, 1997; Zhao et al., 2011a).

23 To demonstrate the latitudinal distribution morphology, stratification events obtained from  
24 continual orbit tracks observed in one day and different days are given in Fig.4 and Fig.5. In both  
25 figures, red and blue color represent data from Swarm A and Swarm B respectively. Stratification  
26 events are located on the places where measurements from Swarm B are greater than that from  
27 Swarm A, namely on places where blue color curves are above red color ones. Also given in Fig.  
28 4(b) are the ground tracks of the two satellites, which can be used to locate the longitude of the  
29 stratification events.

30 As shown in Fig.4(a) and Fig.5(a), morphology of the nighttime stratification events, located near  
31 the geomagnetic equator, shows that the stratification is centered at the equator ionization anomaly  
32 (EIA) trough, where the geomagnetic equator is located at or near for most event cases, and extend  
33 towards the EIA crests on both hemisphere. Occurrence of the nighttime phenomenon can be  
34 accompanied by or without plasma depletion as shown in Fig.4(a) and Fig.5(a). Stratification can  
35 be seen clearly from the satellite measurements even if there are plasma bubbles, whereas it cannot  
36 be easily identified from ground-based ionograms under this disturbed situation. Latitudinal  
37 distribution of this phenomenon indicates that most of the nighttime stratification can cover all the  
38 regions between the two EIA crests, which is quite different from the locations of daytime  
39 stratification, where the occurrence position is near, but not the geomagnetic equator (Balan et al.,  
40 1998; Bastita et al., 2001; Uetomo et al., 2011).

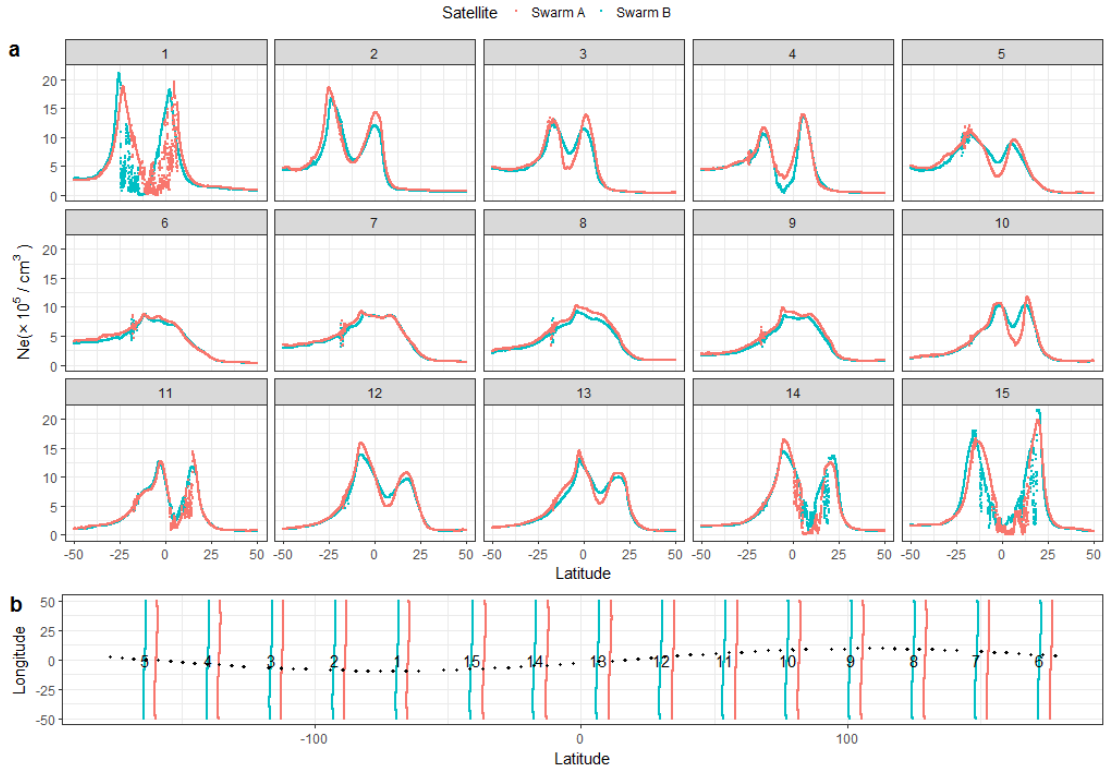


Fig. 4 Morphology of nighttime stratification examples from continual orbit tracks

(a) Morphology of nighttime stratification from continual orbits on 2014-02-03; (b) Ground tracks corresponding to the continual orbit in (a). The dot line in (b) indicates the geomagnetic equator from dipole coordinate and numbers on the line corresponds to the numbers shown in (a).

We also give some examples in Fig.5(b) to show the typical morphology for daytime stratification. These latitudinal distribution morphologies demonstrate clearly the results, reported by many ground-based studies, that daytime stratification can appear on one side, frame 1 and 2 in Fig.5(b), or both sides, frame 4 in Fig.5(b), of the EIA crests. We also show an example of the daytime stratification centered at the EIA trough, frame 3 in Fig.5(b), which is seldom observed from ground-based ionograms. An interesting point in daytime data is that there is a small spike centered at the EIA trough occasionally as shown by frame 4 in Fig.5(b), which is never seen in nighttime measurements and needs further confirmation. As there are only a few daytime stratification events, no statistical results can be obtained from these data. We only focus on nighttime stratification in this study.

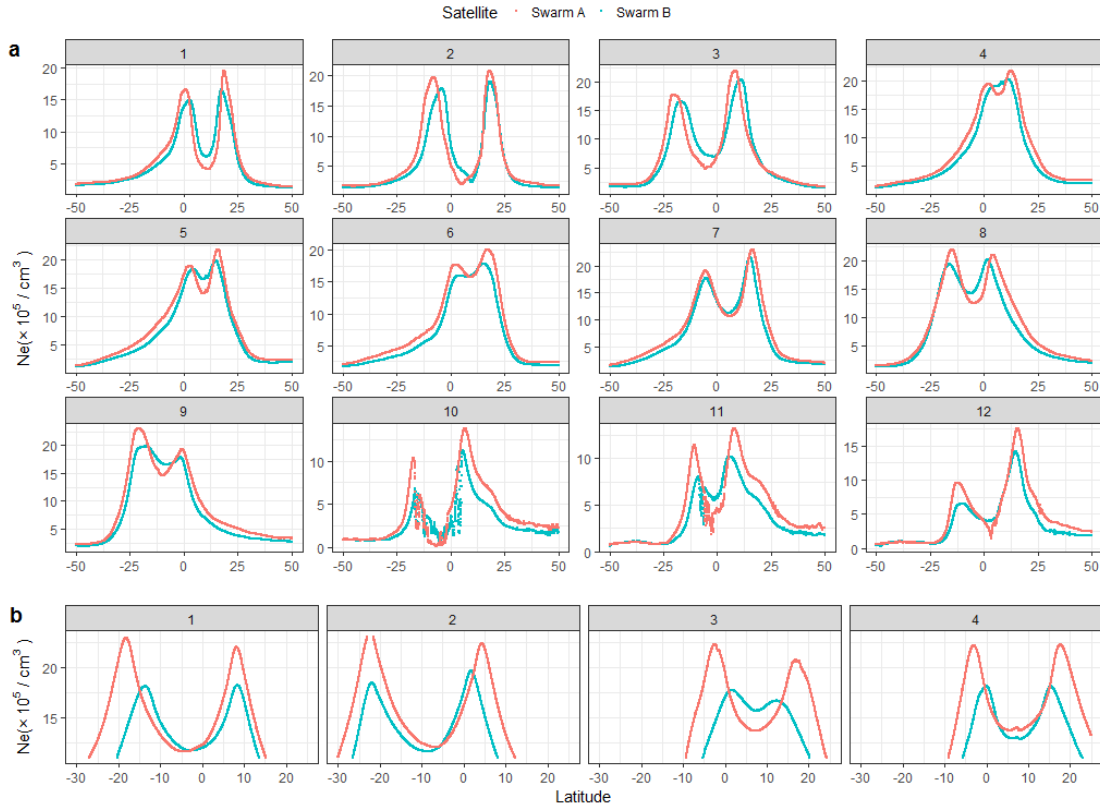


Fig. 5 Morphology of stratification examples from different LT

(a) Morphology of nighttime stratification from different LTs. Figures 1-3 are from 2014-02-12 with LT 19:20; figures 4-9 are from 2014-02-28 with LT 17:50; and figures 10-12 are from 2014-06-12 with LT 21:00; (b) Typical morphology of daytime stratification; Figures 1-2 is from 2014-04-22 with LT about 13:40, figure 3 is from 2014-03-22 with LT 16:00, and figure 4 is from 2014-03-20 with LT about 16:20.)

There is another southern mid-latitude regions where the detected stratification events are concentrated on and can cover all the longitudes as shown in Fig.3(a). Stratification phenomenon in this region is never mentioned in previous studies. All the detected stratification events in this region occur at local nighttime in May and June as mentioned above. Typical stratification events in this region are located on the local plasma peak along latitudinal direction, which is sandwiched by two lower density strips as shown in Fig. 6. Stratification events in this region can occur simultaneously with that located near the geomagnetic equator region as indicated by frame 11 and 12 in Fig.6. The morphology and locations of the stratification events in southern mid-latitudes are quite different from that in geomagnetic equator region, which may imply the different formation mechanism for the two situations.

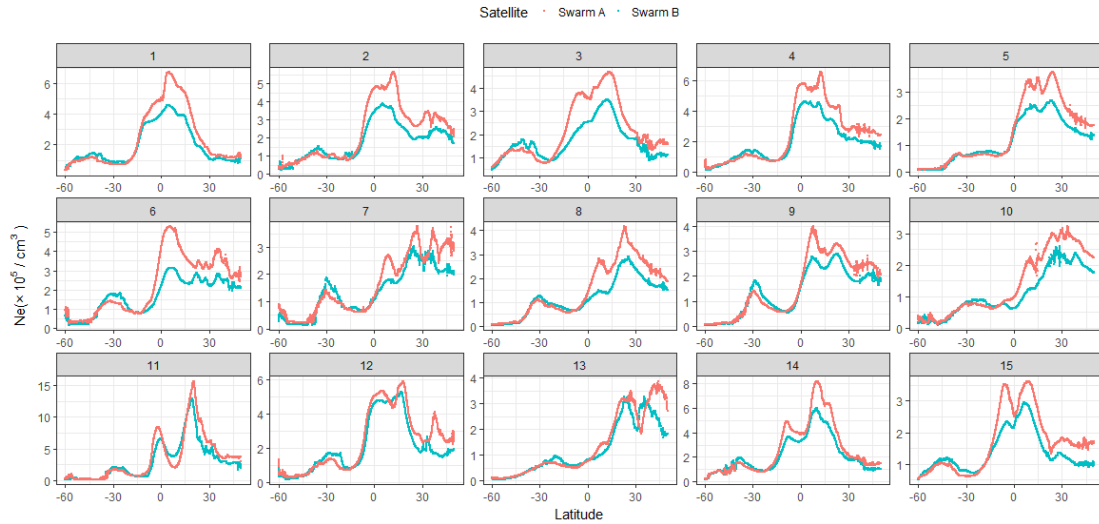


Fig. 6 Examples of stratification in southern mid-latitudes

#### 4. Discussion

To get the peak height range of the ionospheric F2 layer during the selected data period, a statistical analysis is performed using the radio occultation (RO) measurements from the COSMIC mission. Of all the 16753 RO events located between  $\pm 20^\circ$  geographical latitude, only 994 events have peak height greater than 450km, including those with false peak height caused by disturbed data, which indicates that the normal F2 peak height is lower than 450km at the equatorial region. A small number of RO events, located along geomagnetic equator with a higher peak height, show the morphology of two peaks on the profiles, which may imply stratification phenomenon. Therefore, we can determine that the orbiting altitudes of the Swarm satellites are above the F2 peak height for most cases, and the stratification events, appearing at the orbiting altitudes, can be detected by the in situ plasma density measurements from the Swarm satellites.

The continuous morphology of the stratification and its global distribution obtained in this paper give us a more intuitive image of the stratification phenomenon and are very useful to understand this phenomenon. But some problems requires further analysis.

Stratification events detected in this study are mainly concentrated during nighttime period, which is different from previous studies that occurrence of stratification is mainly during daytime, especially during morning to noon period when the stratification are most frequently observed from ground-based ionograms (Balan et al., 1998; Jenks et al., 1997; Batista et al., 2001). As to the reason why daytime stratification events are fewer for the Swarm measurements, a possible reason is that the altitude of the F2 peak and the stratification (F3 layer) are higher during the day than they are at night. Karpachev et al. (2013) demonstrate that the F3 layer height increases from  $\sim 450$ km in the early morning to 600-750km in the afternoon, and Balan et al. (1997) also suggest that the daytime F3 layer occurs above 550km, all of which exceed the orbiting altitudes of the Swarm satellites. As a result, only a few daytime stratification events can be observed. This is also the reason why there are only a few events during March and April as the orbiting LTs of the two satellites are both during the day during this two months. In fact, nighttime stratification is suggested to be a permanent phenomenon by studies using satellite-based ionograms (Depuev and Pulinets, 2001; Lockwood and Nelms, 1964; Uemoto et al., 2011), the results obtained from the Swarm



1 satellites in this paper support this suggestion.

2 Using the measurements of the Swarm satellites, the continuous latitudinal morphology and the  
3 exact locations of the stratification events are shown clearly for the first time, which demonstrate  
4 that the nighttime stratification can cover all the latitudes continuously between the two EIA crests  
5 with the most significant part being located at the EIA trough. This arch-like distribution  
6 morphology is in accord with those studies using satellite-based observations (Depuev and Pulinets,  
7 2001; Lockwood and Nelms, 1964; Wang et al., 2019). Depuev and Pulinets (2001) suggest that the  
8 intensity of the stratification has a maximum just above the equator and decreases poleward within  
9  $\pm 10^\circ$  dip; and Lockwood and Nelms (1964) also report that the field-aligned ledge is concentrated  
10 above the geomagnetic equator, producing a dome-like cross-section in the equatorial region. Wang  
11 et al. (2019) also suggest an arch-like distribution of the nighttime stratification. This feature is quite  
12 different from the daytime stratification, which is more probable at low latitudes around the equator,  
13 rather than at the equator itself (Balan et al., 1998; Batista et al., 2003; Uemoto et al., 2011; Zhao et  
14 al., 2011b); and this location feature is demonstrated clearly by the typical daytime morphology in  
15 Fig.5(b). In contrast, the morphology of most nighttime stratification suggest that the most  
16 significant part is located at the EIA trough rather than at low latitudes on both sides. The different  
17 features of locations and distribution morphology may suggest different formation mechanism for  
18 nighttime and daytime stratification.

19 According to the widely accepted suggestion by Balan et al. (1998), daytime stratification (F3  
20 layer) in equatorial region is formed due to the combined effect of the upward  $E \times B$  drift and neutral  
21 wind; the upward plasma drift causes the F2 peak to drift upward and form F3 layer while the normal  
22 F2 layer develops at lower altitudes through the usual photochemical and dynamical effects. They  
23 also suggest that the upward plasma drift due to the pre-reversal enhancement (PRE) cannot form  
24 stratification because of the absence of the ionization production after sunset, which is later denied  
25 by Zhao et al. (2011a) due to the existence of post-sunset stratification. Their observations show  
26 that post-sunset stratification is different from daytime stratification due to the different solar  
27 activity and season dependence features and they suggest that post-sunset stratification is formed  
28 due to the PRE upward plasma lifts and the existence of ionization production at the high altitudes  
29 of F2 layer after sunset. However, this formation mechanism cannot explain the midnight/post-  
30 midnight stratification shown in this study and mentioned in previous studies (Depuev and Pulinets,  
31 2001; Uemoto et al., 2011), we therefore deduce that nighttime stratification may be resulted from  
32 a different formation mechanism. According to some studies (Balan et al., 2008; Paznukhov, 2007),  
33 the mechanism responsible for the storm time stratification is similar to that in quiet periods but  
34 with a much faster processing time due to the rapid uplift of the F layer by an upward  $E \times B$  drift  
35 resulting from an eastward penetration electric field. We therefore speculate that the upward plasma  
36 drift caused by the PRE will produce the same effects as that of the magnetic disturbances. As a  
37 result, plasma can be lifted up quickly by the PRE from lower altitudes to higher altitudes, which  
38 can lead to the higher densities at higher altitudes and plasma depletion and plasma bubbles at lower  
39 altitude. After the PRE, the downward vertical drift resulting from the reversal electric field will  
40 replenish the depleted region by carrying the plasma from higher altitudes to lower altitude, as a  
41 result stratification can be formed during the downward carrying process at the EIA trough. At the  
42 same time, the field aligned diffusion of the uplifted plasma can maintain the EIA structure on both  
43 sides of the geomagnetic equator and form stratification at low latitudes. By this way, the nighttime  
44 stratification morphology, centering at EIA trough and extending towards the two EIA crests as

1 shown in Fig.4(a) and Fig.5(a), can be formed. The EIA structure, which accompanies all the cases  
2 of stratification near geomagnetic equator, is supposed to be the necessary condition to form the  
3 stratification in this region. The existence of nighttime EIAs is common during geo-magnetically  
4 quiet conditions, and re-appearance of EIA is triggered by the occasionally reversed upward vertical  
5 plasma drift as nighttime vertical velocities are normally directed downwards (Yizengaw et al.,  
6 2009). In addition, the nighttime downward vertical velocities are greater after midnight than before  
7 midnight, both during magnetically quiet and perturbed times (Rajarm, 1977). Combining these  
8 results, we can explain the formation process of the nighttime stratification at and near geomagnetic  
9 equator and why most of the nighttime stratification events are concentrated between post-sunset to  
10 midnight period as shown in Fig.3(c). In addition, according to Balan et al. (2000), variations of  
11 daytime stratification arise from variations of the vertical plasma drift velocities due to the F region  
12 zonal electric field. Similarly, the variations of the nighttime stratification may be related to the  
13 variations of the PRE amplitude, variations of the upward and downward vertical velocities, as well  
14 as variations of the frequency of the EIA re-appearance.

15 The new discovery in this study is the stratification on the southern mid-latitudes, which has never  
16 been mentioned in previous studies. Wang et al. (2019) propose that a small stratification may exist  
17 on southern mid-latitudes when comparing the in situ electron densities observed at different  
18 altitudes by the same payload onboard DEMETER satellite, but a definite conclusion cannot be  
19 given as the data is not observed simultaneously. The results in this paper further confirm their  
20 proposal. However, we also notice that the season and solar activity of the data used in their study  
21 are different from that in this study. Whether stratification on southern mid-latitudes can occur in  
22 all seasons or only in summer (Wang et al., 2019) or winter (in this study), both their studies and  
23 ours cannot give a definite answer due to the limit data coverage, which requires further studies  
24 when enough data are obtained. Zhao et al. (2011b) notice that there are a few cases of stratification  
25 that are far away from the geomagnetic equator in their global stratification distribution obtained  
26 from COSMIC RO data, they attribute it to the result of the propagation of atmospheric gravity  
27 waves (AGWs) often observed in mid-latitudes. We don't think their cases are similar as ours as  
28 their cases are distributed randomly on both hemisphere. As no literatures can be referenced on the  
29 stratification located in the southern mid-latitudes, a brief discussion on its possible formation  
30 mechanism is given here.

31 As shown in Fig.6, stratification events in this region are located on the local plasma peak, and it  
32 seems that the more obvious the local peak is, the more obvious the stratification is. Plasma  
33 enhancement in southern mid-latitudes is noticed by Tsurutani et al. (2004). They call the local peak  
34 "shoulder", and this "shoulder" can be found from TOPEX, SAC-C, and CHAMP data sets, as well  
35 as ground GPS data. Yizengaw et al. (2009) also report TEC enhancement in southern mid-latitudes  
36 and attribute it to the meridional thermospheric wind that drives the F layer plasma upward as this  
37 is the region where the wind-induced uplifting is most efficient. The morphology of the daytime  
38 "shoulder" is similar as the nighttime TEC enhancement and local peak in this study. As this local  
39 peak can exist both during the day and at night as well as under geomagnetic disturbed and quiet  
40 conditions, we suppose that it is a normal phenomenon on southern mid-latitudes. Another  
41 interesting feature from the study of Tsurutani et al. (2004) is the "shoulder" occurs only on Southern  
42 Hemisphere, similar as the feature that mid-latitudes stratification occur only on Southern  
43 Hemisphere. We speculate that the stratification in southern mid-latitudes is closely related with the  
44 local peak structure according to their common feature. Tsurutani et al. (2004) suppose the "shoulder"

1 is likely the signature of the plasmopause, which can be used as a downward plasma source to form  
2 the stratification in the mid-latitudes, but this cannot explain why this phenomenon doesn't appear  
3 in northern mid-latitudes.

4 Abdu et al. (2005) suggest that precipitation of low energy (<10 keV) electrons in the SAA  
5 (South Atlantic Anomaly), namely source of ion production, together with the ionization loss  
6 process, might be a mechanism for the F2 layer stratification at mid-latitudes, but the locations of  
7 their stratification are on the southern EIA crest, quite different from the locations in this study.  
8 Moreover, precipitation mechanism cannot explain why the stratification can cover all the  
9 longitudes.

10 According to Lin et al. (2005), large (storm time) upward  $E \times B$  drifts can lift the ionospheric layer  
11 to higher altitudes, and therefore can expand the EIA peaks to higher latitudes. However, the  
12 proposal, transporting of equatorial plasma to higher geomagnetic latitudes by the super fountain  
13 effect, still cannot satisfactorily explain the stratification in southern mid-latitudes. For one reason,  
14 field-aligned diffusion of the uplift plasma by super fountain may lead to the mid-latitude  
15 stratification, but it cannot explain the trough between the local peak and the southern EIA crest as  
16 shown in Fig.6; the second reason, when there is no EIA signature near the geomagnetic equator,  
17 and as a result no super fountain effect, there are still many stratification cases in this region; and  
18 the third reason, this mechanism cannot explain the absence of stratification in northern mid-  
19 latitudes either. As no existing research results can satisfactorily explain the formation mechanism  
20 of the stratification in southern mid-latitudes, we put it as an open question here, and subsequent  
21 studies are anticipated.

## 22 5. Summary

23 Stratification above F2 peak is investigated in this paper using the continuous in situ plasma  
24 densities observed simultaneously by the Swarm satellites orbiting at different altitudes, some  
25 refined features and new discovery on the F2 layer stratification are summarized as follows:

- 26 (1) It is the first time that stratification phenomenon is investigated using direct in situ plasma  
27 density measurements.
- 28 (2) Most of the detected stratification events occur after sunset, and cluster between about 18:00  
29 to 23:00 LT.
- 30 (3) The continuous morphology of the nighttime stratification events, located near geomagnetic  
31 equator, shows that it centers at the EIA trough and extends towards both sides, but  
32 sandwiched by the two EIA crests. This distribution feature is quite different from the  
33 daytime stratification, which is located near but not the equator.
- 34 (4) A new discovery is found that some detected nighttime stratification events are concentrated  
35 near mid geomagnetic latitudes on Southern Hemisphere along all the longitudes, and the  
36 stratification in this region is found to be located on the local plasma peak. Further studies  
37 are expected on its formation mechanism.

## 38 Acknowledgment

39 This work was supported by the National Key R&D Program of China (Grant  
40 no.2018YFC1503505). The plasma density data (LP) of the Swarm satellites can be downloaded

1 from <https://earth.esa.int/>. The Dst data was downloaded from <http://wdc.kugi.kyoto-u.ac.jp>, and  
2 the F107 and Sunspot data were downloaded from <ftp://ftp.ngdc.noaa.gov>.

### 3 Reference

4 Abdu, M. A., Batista, I. S., Carrasco, A. J., and Brum, C. G. M.: South Atlantic magnetic anomaly ionization: A  
5 review and a new focus on electrodynamic effects in the equatorial ionosphere. *Journal of Atmospheric and Solar-*  
6 *Terrestrial Physics*, 67(17-18), 1643–1657, doi:10.1016/j.jastp.2005.01.014, 2005.

7 Balan, N., Bailey, G. J., Abdu, M. A., Oyama, K. I., Richards, P. G., MacDougall, J., and Batista, I. S.: Equatorial  
8 plasma fountain and its effects over three locations: Evidence for an additional layer, the F3 layer. *Journal of*  
9 *Geophysical Research: Space Physics*, 102(A2), 2047–2056, doi:10.1029/95ja02639, 1997.

10 Balan, N., Batista, I. S., Abdu, M. A., MacDougall, J., and Bailey, G. J.: Physical mechanism and statistics of  
11 occurrence of an additional layer in the equatorial ionosphere. *Journal of Geophysical Research: Space Physics*,  
12 103(A12), 29169–29181, doi:10.1029/98ja02823, 1998.

13 Balan, N., Batista, I. S., Abdu, M. A., Bailey, G. J., Watanabe, S., MacDougall, J., and Sobral, J. H. A.: Variability  
14 of an additional layer in the equatorial ionosphere over Fortaleza. *Journal of Geophysical Research: Space Physics*,  
15 105(A5), 10603–10613, doi:10.1029/1999ja000020, 2000.

16 Balan, N., Thampi, S. V., Lynn, K., Otsuka, Y., Alleyne, H., Watanabe, S., Abdu, M. A., and Fejer, B. G.: F3 layer  
17 during penetration electric field. *Journal of Geophysical Research: Space Physics*, 113(A3), A00A07,  
18 doi:10.1029/2008ja013206, 2008.

19 Batista, I. S., Abdu, M. A., MacDougall, J., and Souza, J.: Long term trends in the frequency of occurrence of the  
20 F3 layer over Fortaleza, Brazil. *Journal of Atmospheric and Solar-Terrestrial Physics*, 64(12-14), 1409–  
21 1412, doi:10.1016/s1364-6826(02)00104-9, 2002.

22 Depuev, V. H., and Pulinets, S. A.: Intercosmos-19 observations of an additional topside ionization layer: the F3  
23 layer. *Advances in Space Research*, 27(6-7), 1289–1292, doi:10.1016/s0273-1177(01)00205-8, 2001.

24 Fagundes, P. R., Klausner, V., Sahai, Y., Pillat, V. G., Becker-Guedes, F., Bertoni, F. C. P., Bolzan, M. J. A., and  
25 Abalde, J. R.: Observations of daytime F2-layer stratification under the southern crest of the equatorial ionization  
26 anomaly region. *Journal of Geophysical Research: Space Physics*, 112(A4), A04302, doi:10.1029/2006ja011888,  
27 2007.

28 Jenkins, B., Bailey, G. J., Abdu, M. A., Batista, I. S., and Balan, N.: Observations and model calculations of an  
29 additional layer in the topside ionosphere above Fortaleza, Brazil. *Annales Geophysicae*, 15(6), 753–759,  
30 doi:10.1007/s00585-997-0753-3, 1997.

31 Karpachev, A. T., Klimenko, M. V., Klimenko, V. V., and Kuleshova, V. P.: Statistical study of the F3 layer  
32 characteristics retrieved from Intercosmos-19 satellite data. *Journal of Atmospheric and Solar-Terrestrial Physics*,  
33 103, 121–128, doi:10.1016/j.jastp.2013.01.010, 2013.

34 Knudsen, D. J., Burchill, J. K., Buchert, S. C., Eriksson, A. I., Gill, R., Wahlund, J.-E., Ahlen, L., Smith, M., and Moffat,  
35 B.: Thermal ion imagers and Langmuir probes in the Swarm electric field instruments. *Journal of Geophysical Research: Space*  
36 *Physics*, 122, 2655-2673, doi:10.1002/2016ja022571, 2017.

37 Lin, C. H., Richmond, A. D., Heelis, R. A., Bailey, G. J., Lu, G., Liu, J. Y., Yeh, H. C., and Su, S.-Y.: Theoretical  
38 study of the low- and midlatitude ionospheric electron density enhancement during the October 2003 superstorm:  
39 Relative importance of the neutral wind and the electric field. *Journal of Geophysical Research*, 110,  
40 A12312, doi:10.1029/2005ja011304, 2005.

41 Lockwood, G. E. K., and Nelms, G. L.: Topside sounder observations of the equatorial anomaly in the 75° W  
42 longitude zone. *Journal of Atmospheric and Terrestrial Physics*, 26(5), 569–580, doi:10.1016/0021-9169(64)90188-

1 6, 1964.

2 Lomidze, L., Knudsen, D. J., Burchill, J., Kouznetsov, A., and Buchert, S. C.: Calibration and Validation of Swarm  
3 Plasma Densities and Electron Temperatures Using Ground-Based Radars and Satellite Radio Occultation  
4 Measurements. *Radio Science*, 53(1), 15–36, doi:10.1002/2017rs006415, 2018.

5 Paznukhov, V. V., Reinisch, B. W., Song, P., Huang, X., Bullett, T. W., and Veliz, O.: Formation of an F3 layer in  
6 the equatorial ionosphere: A result from strong IMF changes. *Journal of Atmospheric and Solar-Terrestrial Physics*,  
7 69(10-11), 1292–1304, doi:10.1016/j.jastp.2006.08.019, 2007.

8 Rajaram, G.: Structure of the equatorial F-region, topside and bottomside—a review. *Journal of Atmospheric and*  
9 *Terrestrial Physics*, 39(9-10), 1125–1144, doi:10.1016/0021-9169(77)90021-6, 1977.

10 Sen, H. Y.: Stratification of the F2-layer of the ionosphere over Singapore. *Journal of Geophysical Research*, 54(4),  
11 363–366, doi:10.1029/jz054i004p00363, 1949.

12 Skinner, N. J., Brown, R. A., and Wright, R. W.: Multiple stratification of the F-layer at Ibadan. *Journal of*  
13 *Atmospheric and Terrestrial Physics*, 5(1-6), 92–100, doi:10.1016/0021-9169(54)90013-6, 1954.

14 Shim, J. S., Scherliess, L., Schunk, R. W., and Thompson, D. C.: Spatial correlations of day-to-day ionospheric  
15 total electron content variability obtained from ground-based GPS, *Journal of Geophysical Research: Space Physics*,  
16 113, A09309, doi:10.1029/2007ja012635, 2008.

17 Thampi, S. V., Ravindran, S., Devasia, C. V., Pant, T. K., Sreelatha, P., and Sridharan, R.: First observation of  
18 topside ionization ledges using radio beacon measurements from low Earth orbiting satellites, *Geophys. Res. Lett.*,  
19 32, L11104, doi:10.1029/2005GL022883, 2005.

20 Tsurutani, B., Mannucci, A., Iijima, B., Abdu, M. A., Sobral, J.H.A., et al. (2004). Global dayside ionospheric  
21 uplift and enhancement associated with interplanetary electric fields. *Journal of Geophysical Research*,  
22 109(A8). doi:10.1029/2003ja010342

23 Uemoto, J., Ono, T., Kumamoto, A., and Iizima, M.: Statistical analysis of the ionization ledge in the equatorial  
24 ionosphere observed from topside sounder satellites. *Journal of Atmospheric and Solar-Terrestrial Physics*, 68(12),  
25 1340–1351, doi:10.1016/j.jastp.2006.05.015, 2006.

26 Wang, X., Yang, D., Liu, D., and Chu, W.: Identifying a possible stratification phenomenon in ionospheric F2  
27 layer using the data observed by the DEMETER satellite: method and results. *Annales Geophysicae*, 37(4), 645–  
28 655, doi:10.5194/angeo-37-645-2019, 2019.

29 Yizengaw, E., Moldwin, M. B., Sahai, Y., and de Jesus, R.: Strong postmidnight equatorial ionospheric anomaly  
30 observations during magnetically quiet periods. *Journal of Geophysical Research: Space Physics*, 114(A12),  
31 RS6004, doi:10.1029/2009ja014603, 2009.

32 Zhao, B., Wan, W., Reinisch, B., Yue, X., Le, H., Liu, J., and Xiong, B.: Features of the F3 layer in the low-latitude  
33 ionosphere at sunset. *Journal of Geophysical Research: Space Physics*, 116(A1), A01313, doi:10.1029/2010ja016111,  
34 2011a.

35 Zhao, B., Wan, W., Yue, X., Liu, L., Ren, Z., He, M., and Liu, J.: Global characteristics of occurrence of an  
36 additional layer in the ionosphere observed by COSMIC/FORMOSAT-3. *Geophysical Research Letters*, 38(2),  
37 L02101, doi:10.1029/2010gl045744, 2011b.